

Spectral Analysis of Nonstationary Dynamics

By Gary Froyland

$$\mathcal{L}f = f \circ T^{-1}.$$

Fluid mixing is key to many man-made and natural processes, such as food and mineral processing, paint manufacture, blood flow, micro-electronic heat exchange, the propulsion of aquatic animals, and the dynamics of Earth's ocean and atmosphere. Scientists and engineers are increasingly able to use experimental techniques—like particle-tracking velocimetry and laser-induced fluorescence—to observe the fine fluid motions that bring about mixing. Here I outline some mathematical approaches to analyse and manipulate transport and mixing caused by autonomous and time-dependent dynamics.

Transport and Mixing

Broadly speaking, transport is the bulk movement of parcels of fluid within the fluid domain, and mixing refers to the extent of these parcels' intertwining over time. Figure 1 displays four frames of carbon dioxide levels in Earth's atmosphere, spaced a couple of days apart.

For the purposes of illustration, let's overlook the fact that carbon dioxide is continually injected and removed from the atmosphere. Over a period of eight days, there is considerable change in the location of carbon dioxide peaks (red) in Figure 1; these peaks have been transported. The overall carbon dioxide distribution also changes. In the absence of carbon dioxide injection and removal, one would expect the distribution to begin "evening out" due to mixing processes.

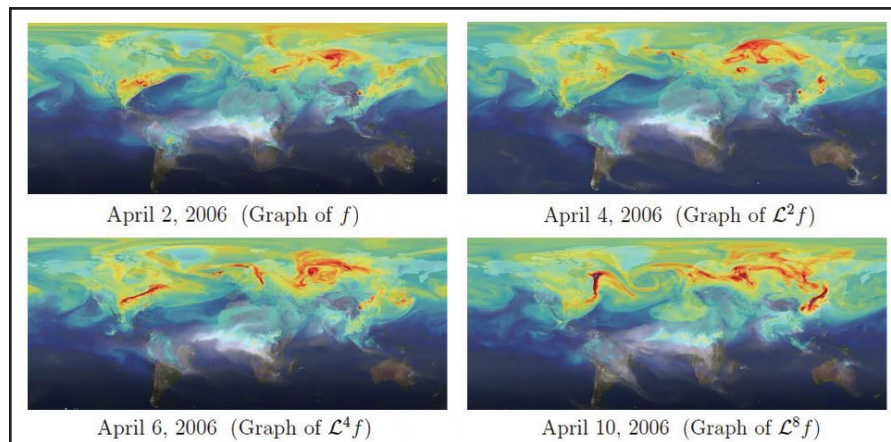


Figure 1. Stills from NASA's "A Year in the Life of Earth's CO₂." See <http://svs.gsfc.nasa.gov/goto?11719> for more detail.

The Transfer Operator

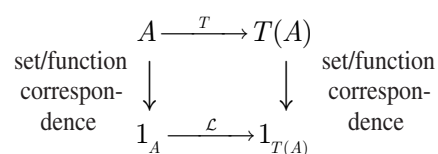
A simple linear operator—associated with the nonlinear dynamics—can conveniently analyse transport and mixing in the phase space X of a nonlinear dynamical system $T: X \rightarrow X$. This linear operator \mathcal{L} is the transfer operator [8] and acts on real functions $f: X \rightarrow \mathbb{R}$. It is a composition operator, and for invertible volume-preserving dynamics in particular, is simply composition with the backward-time nonlinear dynamics:

For the dynamics of compressible fluids, the transfer operator includes an additional scaling term to ensure that $\mathcal{L}f$ is a density if $f: X \rightarrow \mathbb{R}$ is a density. For demonstration purposes, assume that the wind field is unchanging over eight days, X is the domain shown in Figure 1, and $T: X \rightarrow X$ describes the daily evolution of air particles. If the initial concentration of carbon dioxide is given by a density f , then the figures at April 4, April 6, and April 10 are graphs of $\mathcal{L}^2 f$, $\mathcal{L}^4 f$, and $\mathcal{L}^8 f$ respectively.

Why composition with T^{-1} ? Suppose we wish to track the transport of a subset $A \subset X$ under an invertible volume-preserving map T . We can identify the set A with function 1_A , which takes the value 1 on A and the value 0 outside A . Then

$$\mathcal{L}1_A = 1_A \circ T^{-1} = 1_{T(A)}.$$

Thus, the forward-time image of 1_A under \mathcal{L} leads to the function $1_{T(A)}$, identified with $T(A)$, the forward image of A under T . The following diagram summarises this set/function correspondence.



Therefore, we can use the transfer operator to linearly evolve the functional representation of a set forward in time. This functional approach is richer than the con-

sideration of sets because we may employ the transfer operator to evolve concentrations of quantities forward in time (see Figure 1, on page 1). The transfer operator is thus an extremely convenient tool for studying transport; the same is true of the analysis of mixing properties.

The Spectrum and Mixing

The transfer operator is a Markov operator because of (i) positivity: $f \geq 0 \Rightarrow \mathcal{L}f \geq 0$ and (ii) integral preservation: $\int f(x) dx = \int \mathcal{L}f(x) dx$. By anal-

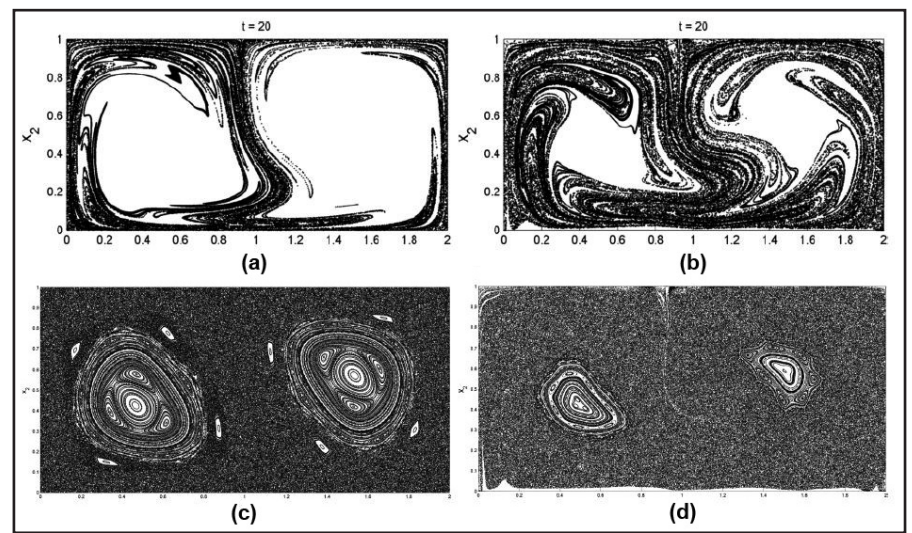


Figure 3. Enhancing mixing in the double gyre flow. **3a.** Evolution of a small parcel of fluid for 20 periods of the double gyre flow [9]. **3b.** Evolution of the same parcel of fluid after manipulation of the spectrum to increase mixing. **3c.** Poincaré map of the double gyre flow. **3d.** Poincaré map of the slightly perturbed flow. Images courtesy of [6].

ogy to stochastic transition matrices of mixing (irreducible and aperiodic) Markov chains, where the second-largest eigenvalue λ_2 of the transition matrix controls the exponential rate of mixing, the second eigenvalue λ_2 of \mathcal{L} also controls the rate of mixing in phase space X . Several different mathematical setups can formalise this idea, such as selecting the Banach space \mathcal{B} to be compatible with the dynamics T [1] or adding a small amount of diffusive noise to T and setting \mathcal{B} to $L^1(X)$, for example. Either way, the transfer operator possesses a spectral gap between the leading eigenvalue 1 (with eigenfunction

Nonstationary, Nonautonomous, and Time-dependent Dynamics

What can one do when the dynamics is nonstationary or nonautonomous, where the governing dynamics changes over time—as is the case in the atmosphere, where the wind field today may be very different from the wind field tomorrow? If a sequence of maps $T_1: X \rightarrow X$, $T_2: X \rightarrow X$, ..., $T_n: X \rightarrow X$, ..., describes the nonstationary dynamics, one can study the phase space transport using the composition

$$\dots \mathcal{L}_{T_n} \circ \dots \circ \mathcal{L}_{T_2} \circ \mathcal{L}_{T_1}.$$

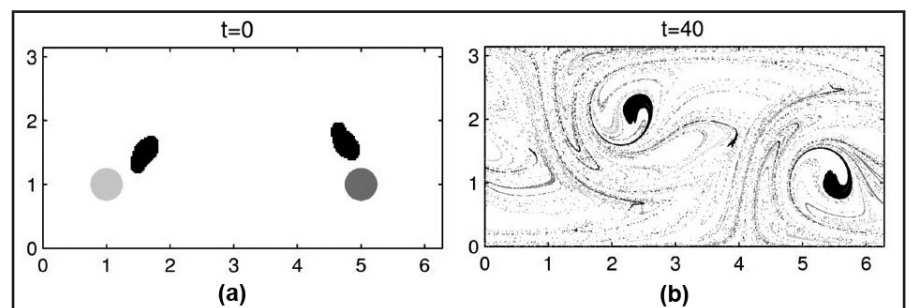


Figure 4. A time-dependent flow on a cylinder. **4a.** Black sets are identified as coherent sets and grey sets are chosen arbitrarily. **4b.** After a lengthy evolution time, the black sets remain largely coherent while the grey sets have readily mixed with the rest of the phase space. Images courtesy of Gary Froyland and Naratip Santitissadeekorn.

the invariant density of T) and retains a well-defined exponential rate of mixing, given by $|\lambda_2|$ (see Figure 2a). The eigenfunction corresponding to λ_2 encodes the almost-invariant sets [2] responsible for the mixing rate (see Figure 2b).

Spectral Manipulation to Optimize Mixing

One can exploit the spectral picture in Figure 2 to optimally speed up or slow down the rate of mixing [6]. Figure 3 shows the result of manipulating the spectrum to make the second eigenvalue move away from the unit circle. This increases not only the size of the chaotic region in phase space (see Figures 3c and 3d), but also the rapidity of the spread of an initial parcel of dye in fluid (see Figures 3a and 3b).

If we wish to study mixing for these time-dependent dynamics, we must adjust our approach. The notion of "second eigenvalue" does not make sense if the applied transfer operator varies from one time step to the next. The key property related to the second eigenvalue-eigenfunction pair (λ_2, f_2) when the governing dynamics is stationary is the existence of a $C < \infty$, such that $\|\mathcal{L}^n f_2\| \leq C \lambda_2^n \|f_2\|$ for all $n \geq 0$. This expression quantifies the exponential mixing rate of $|\lambda_2|$. We can mimic this property in the time-dependent setting by asking that

$$\|\mathcal{L}_{T_n} \circ \dots \circ \mathcal{L}_{T_2} \circ \mathcal{L}_{T_1} f\| \leq C \lambda_2^n \|f\|$$

for all $n \geq 0$,

or taking logs, dividing by n and sending $n \rightarrow \infty$,

$$\lim_{n \rightarrow \infty} \frac{1}{n} \log \|\mathcal{L}_{T_n} \circ \dots \circ \mathcal{L}_{T_2} \circ \mathcal{L}_{T_1} f\| \leq \log \lambda_2. \quad (1)$$

Formally, $\log \lambda_2$ is a Lyapunov exponent of the cocycle of transfer operators $\dots \mathcal{L}_{T_n} \circ \dots \circ \mathcal{L}_{T_2} \circ \mathcal{L}_{T_1}$ and quantifies the rate of mixing [4]. We either select a Banach space \mathcal{B} or add noise to the dynamics to ensure a (Lyapunov) spectral gap between $\log \lambda_1 = \log 1 = 0$ and $\log \lambda_2 < 1$. The subspace (which is one-dimensional if λ_2 is simple) spanned by f that produces equality in (1) encodes the coherent set at time 0 and is responsible for the mixing rate. Figure 4a shows two black sets, identified as coherent sets, and two nearby grey sets. As time progresses, the black

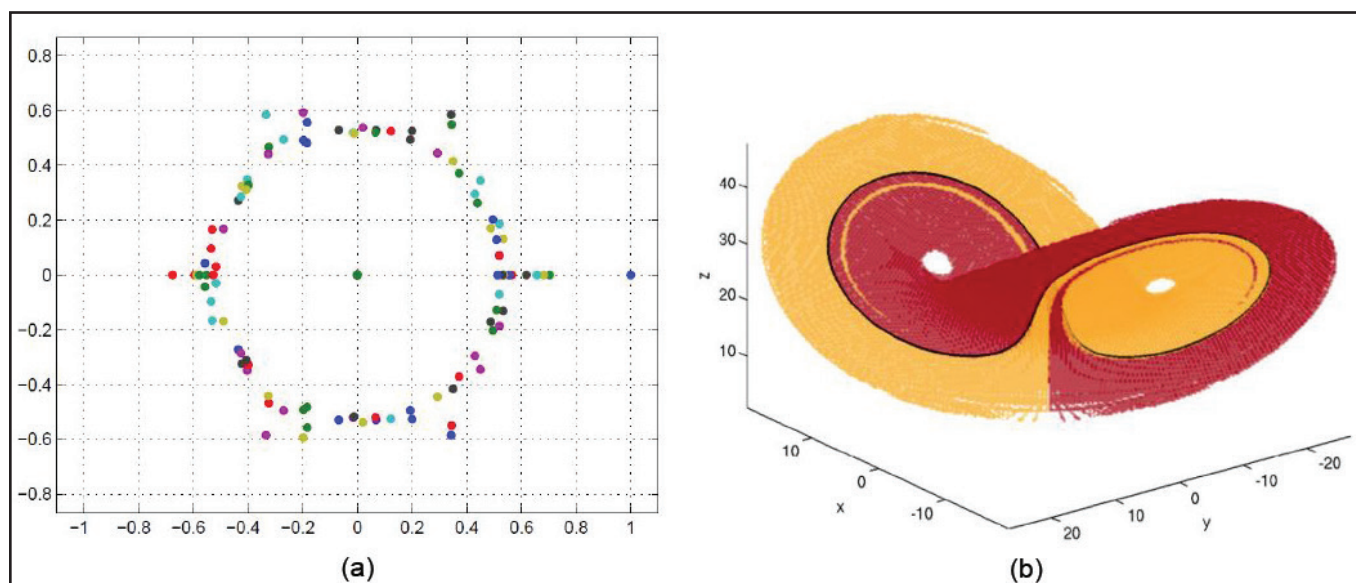


Figure 2. Spectrum and almost-invariant sets. **2a.** Approximation of the largest (in magnitude) eigenvalues, plotted in the complex plane, of the transfer operator for the standard map. Image courtesy of Gary Froyland. **2b.** Computed dominant almost-invariant sets (shown in yellow and red) for the Lorenz system. The black curve identifies the lowest-periodic orbit. Image courtesy of [5].

sets remain largely coherent while the grey sets are quickly mixed into the phase space (see Figure 4b).

Finite-time Dynamics

In many situations, one is concerned with transport and mixing over a finite-time horizon. For example, physical, chemical, and biological systems often have natural timescales that are important for dynamical analyses. We take (1) and truncate time at step n , obtaining

$$\|\mathcal{L}_{T_n} \circ \dots \circ \mathcal{L}_{T_2} \circ \mathcal{L}_{T_1} f\| \leq \lambda_2^n \|f\|. \quad (2)$$

$\mathcal{L}_{T_n} \circ \dots \circ \mathcal{L}_{T_2} \circ \mathcal{L}_{T_1}$ pushes the function f forward under n time steps of the time-dependent dynamics. We wish to find the largest $0 < \lambda_2 < 1$, which is again possible due to the existence of a spectral gap from $\lambda_1=1$. We accomplish this by selecting f as the *singular vector* corresponding to the second-largest singular value of the composition $\mathcal{L}_{T_n} \circ \dots \circ \mathcal{L}_{T_2} \circ \mathcal{L}_{T_1}$ [3, 7]. The singular vector f describes the distribution with the slowest decay or mixing over the finite-time duration $t=1, \dots, n$, and encodes the *finite-time coherent set* responsible for this slow mixing (see Figure 5a and 5b).

References

[1] Baladi, V. (2018). *Dynamical Zeta Functions and Dynamical Determinants for Hyperbolic Maps: A Functional Approach*. In *Ergebnisse der Mathematik und ihrer Grenzgebiete. 3. Folge / A Series of Modern Surveys in Mathematics* (Vol. 48). Springer International Publishing.

[2] Dellnitz, M., & Junge, O. (1999). On the approximation of complicated dynamical behavior. *SIAM J. Numer. Anal.*, 36, 491-515.

[3] Froyland, G. (2013). An analytic framework for identifying finite-time coherent sets in time-dependent dynamical systems. *Phys. D*, 250, 1-19.

[4] Froyland, G., Lloyd, S., & Santitissadeekorn, N. (2010). Coherent sets for nonautonomous dynamical systems. *Phys. D*, 239, 1527-1541.

[5] Froyland G., & Padberg, K. (2009). Almost-invariant sets and invariant manifolds connecting probabilistic and geometric descriptions of coherent structures in flows. *Phys. D*, 238, 1507-1523.

[6] Froyland G., & Santitissadeekorn, N. (2017). Optimal mixing enhancement. *SIAM J. Appl. Math.*, 77, 1444-1470.

[7] Froyland, G., Santitissadeekorn, N., & Monahan, M. (2010). Transport in time-dependent dynamical systems: Finite-time coherent sets. *Chaos*, 20, 043116.

[8] Lasota, A., & Mackey, M.C. (2013). *Chaos, Fractals, and Noise: Stochastic Aspects of Dynamics*. In *Applied Mathematical Sciences* (Vol. 97). New York, NY: Springer.

[9] Shadden, S.C., Lekien, F., & Marsden, J.E. (2005). Definition and properties of Lagrangian coherent structures from finite-time Lyapunov exponents in two-dimensional aperiodic flows. *Phys. D*, 212, 271-304.

Gary Froyland is a professor in the School of Mathematics and Statistics at the University of New South Wales, Sydney, Australia.

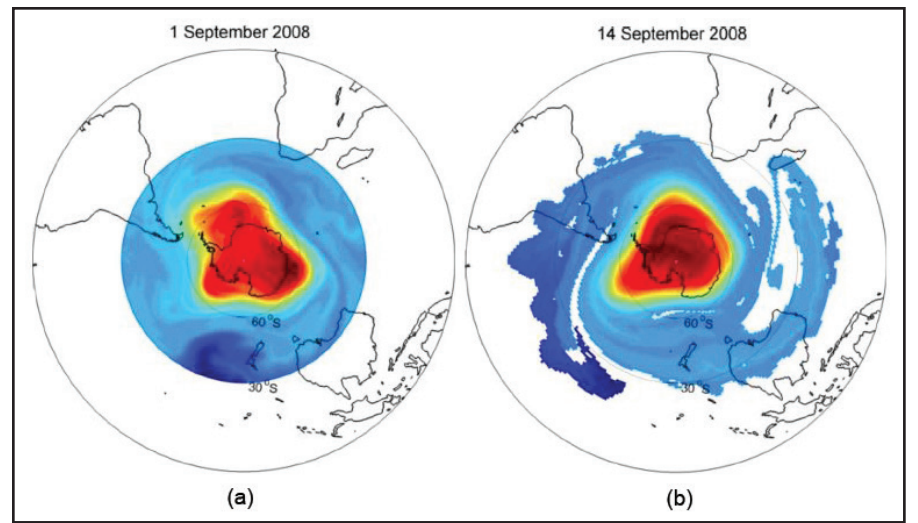


Figure 5. Stratospheric flow over the South Pole. The Antarctic polar vortex is the most coherent set in the region over the polar cap and is identified as red in the second singular vector. **5a.** Left singular vector (on September 1, 2008). **5b.** Right singular vector (on September 14, 2008). Figure courtesy of [7].